The crucial role of diagnostics in achieving ignition on the National Ignition Facility (NIF)

J. D. Kilkenny,[a] A. Pak,[b] O L Landen [b] A. S. Moore,[b] N. B. Meezan,[b] S. W. Haan,[b] W. W. Hsing,[b] S. H. Batha,[c] D. K. Bradley,[b] M. Gatu-Johnson,[e] A. J. Mackinnon,[b] S. P. Regan[d]

a) General Atomics, San Diego, California 92186, USA
b) Lawrence Livermore National Laboratory, Livermore, California 94551-0808, USA
c) Los Alamos National Laboratory, Los Alamos, New Mexico 87545, USA
d) Laboratory for Laser Energetics, University of Rochester, Rochester, New York 14623, USA
e) Plasma Science and Fusion Center, Massachusetts Institute of Technology, Cambridge, Massachusetts 02139, USA

This work performed under the auspices of the U.S. Department of Energy by General Atomics under Contract 89233119CNA000063, by Lawrence Livermore National Laboratory under Contract DE-AC52-07NA27344, by Los Alamos National Laboratory under Contract 89233218CNA, by the Laboratory for Laser Energetics under Award DE-NA0003856, the University of Rochester, and the New York State Energy Research and Development Authority.

Draft IM release number is: LLNL-JRNL-861386-DRAFT

Abstract

Well over 100 diagnostics can operate on the NIF as a result of several decades of development on NIF and before that on Nova, OMEGA and earlier LLNL lasers. A subset of these has guided the approach to achieving ignition on the NIF in 2022[1]. Achieving ignition on NIF has required many types of experiments with this core set of diagnostics, some constraining known unknowns and some revealing surprises, arguably unknown unknowns. Early design work realized that the extreme precision required for ignition on NIF would require fine tuning by experiment, that is, measuring and adjusting known unknowns. Many examples are given where the use of the core set of ignition diagnostics in experimental arrangements called platforms, demonstrated control of the key theoretical parameters defined as shape, adiabat, velocity and mix. The direction of the adjustments to input conditions is found either by trend analysis or in many cases observing from the diagnostic data the direction to make an adjustment. But in addition, diagnostics have revealed some unexpected or neglected known issues which degrade performance, or unexpected issues, unknown unknowns. Some of these factors had been previously considered, but underestimated or difficult to calculate at the time. The overall methodology can be described as a variant of Popper's falsifiability philosophy[2]. This paper summarizes the role of ignition diagnostic in terms of falsification or validation of theory or experimental set up as well as uncovering unexpected issues. The journey to ignition started in the seventies with a 1 μm wavelength laser producing disastrous results. Diagnostics have guided us to the recent multi decadal goal of demonstrating ignition and burn in the laboratory.

1. Introduction

ICF research at the NIF primarily uses laser x-ray drive in which the fusion capsule is surrounded by a high-Z hohlraum which is used to convert laser energy into near symmetric x-ray drive on the capsule. Hot-spot ignition has recently been achieved on NIF by minimizing impurity radiation and thermal conduction losses, so that heating by the α-particles generated in the [D + T $\rightarrow$ n (14.1MeV) + ^{4}He (3.5 MeV)] fusion reaction dominates, and the plasma begins to self-heat, burn, and ignite[1], releasing more energy than the laser energy. Precise measurements of the plasma conditions by x-rays, γ-rays and neutrons observables were key to achieving ignition.

On December 5, 2022, NIF delivered 2.05 MJ of 0.35 μm laser energy to a target that then produced 3.15 MJ of fusion energy (gain of ~1.5)[1]. This ignition was achieved by increasing the laser, radiation drive and coupling efficiency, adjusting the details of the laser/target setup, and improving target quality in terms of material and morphology. Over many years diagnostics showed the changes of design needed to increase drive, improve drive symmetry, shock timing, implosion velocity, and mitigate ablator mix into the hot implosion. Diagnostics suggested further improvement mainly in the target quality needed to reduce observed degradations and achieve ignition.

It has been known for many years that achieving ignition requires optimization of four high-level variables illustrated in Figure 1. These are, shape, adiabat, velocity and mix[3, 4]. In calculations, at least, precisely setting this set of parameters achieves x-ray driven ignition with a NIF sized laser delivering ~ 2MJ of energy to the target. But it was also recognized that the demanding requirements on these four parameters needed for ignition could not be set by calculations alone. In the parlance of this paper these are known unknowns. The experimental setups that would enable the tuning of these known unknowns to achieve ignition are shown in cartoon form on Figure 1. These experimental configurations, called platforms, use the core sets of ignition diagnostics[5, 6]. The discovery of the direction and magnitude of adjustments needed is done through experimental scans which ideally vary (if possible) just one parameter at a time to measure sensitivity slopes and offsets which are compared to simulated or trend analysis[7]. Additionally imaging diagnostics directly show the direction of adjustment. The methodology of measurements validating or falsifying theory is a modification of Popper's parlance[2] as discussed in section 2.

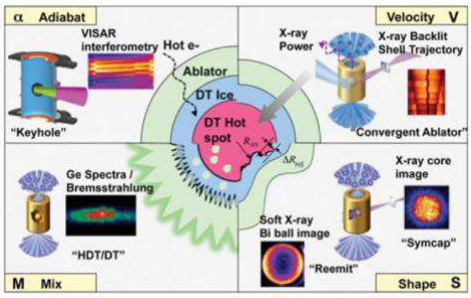

Fig 1. The four crucial parameters to achieve ignition, from reference 3 with permission.

Achieving ignition on NIF was a multi-decade activity involving hundreds of scientists and engineers; diagnostics were crucial to all phases of getting to ignition in monitoring experimental performance and identifying degradation mechanisms and mitigations. Hundreds of scientists and engineers from many institutions have been involved in developing these diagnostics for ignition. NIF emerged from extensive simulations and experimental work on Nova and OMEGA which guided the diagnostics installed on NIF as described in section 3. The effort has been nationally coordinated for many decades by a group currently called the National Diagnostic Working Group [6]. Section 3 is a brief history of these efforts.

The first necessity in achieving ignition is the efficient conversion of laser energy to x-ray drive. Early theory about conversion efficiency with infrared lasers was falsified by diagnostics in the late seventies leading to a multi-decade program with ultra-violet laser light on Nova, OMEGA and NIF. The diagnostics used for these successful radiation temperature measurements are described in section 4 [3,4]. The first of several epochs on NIF, called the National Ignition Campaign (NIC) and the high foot campaigns, sought to measure and control the known unknowns of Figure 1: symmetry, implosion velocity, adiabat and mix. This is described in section 5. Despite separate control of these known unknowns, thermonuclear performance was disappointing. Ignition designs evolved with modifications to target geometry and materials and laser pulse shapes and wavelengths guided by existing and evolving diagnostics. As well as the known unknowns, the above diagnostics discovered unknown unknown degradations which we were able to mitigate as described in section 6, which together with increased drive finally achieved ignition. The several diagnostics used to show that ignition was achieved are described in section 7.

2. The role of diagnostics in ICF

The proximate role of diagnostics in a mission driven activity such as ICF is to measure observables in order to falsify or validate theory, embodied in simulations[2]. Popper proselytized the idea of falsification. In ICF, radiation hydrodynamics as a whole, is not what is being tested for falsification, but ICF models and simulations are. ICF experimentalists perform a series of experiments which are then used to test codes against the observables. This process leads to adjustments to the models or the boundary or initial conditions of the experiments such as the beam balance, time history, wavelength difference or target quality, which hopefully brings models and experiment closer together. This process is more appropriately described as micro-falsification, or micro-validation as shown in Figure 2. Many examples are illustrated in sections 4 & 5. Moreover, measurements can accomplish more than this testing of known

unknowns against our expectations from imprecise theory or experimental setup. Measurements can reveal unknown unknowns or phenomena which were thought of but inaccurately simulated or experimentally prepared. Good examples are "ice" on the laser entrance hole (LEH) window which affected laser burn-in time and the surprising observation of a significant hot spot drift velocity of a burning plasma. Imaging diagnostics in particular can suggest mitigations in observed degradations as discussed in sections 4 & 5.

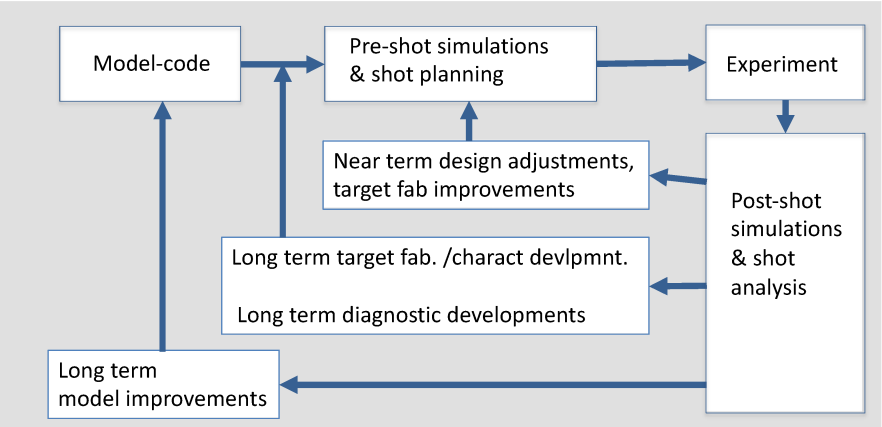

Fig 2. The micro-falsification and micro-validation process used to achieve ignition.

3. The ignition point design guided the choice of the initial NIF diagnostics.

After many years of Nova experiments, diagnostics[8] and code development, NIF emerged in 1994 with the Conceptual Design Report (CDR)[9]. The NIF requirements were based on evolving design work tested or micro-falsified by Nova experiments, identifying some known unknowns for ignitions[10, 11]. In particular it was recognized that shock timing and drive symmetry were known unknowns meaning that models were known not to be accurate enough to achieve the high precision needed for ignition without tuning by experiments. The NIF plans and requirements were heavily reviewed in the period from 1990 to 1996, culminating in the second NAS report in 1997 on ICF[12] which said " *the committee now believes that uncertainties in ignition arise only from considerations of mix, symmetry, and laser-plasma interactions-phenomena that can be studied best in laboratory experiments"*. Based on Nova diagnostics and an early plan to get to ignition, a set of ignition diagnostics for NIF was conceived and allocated amongst the national ignition program. Table 1 lists most of these diagnostics and their functions.

Additional diagnostics were planned, to supplement this basic list. To address non-uniform compressed fuel areal density a set of 17 and then 48 Zr activation detectors respectively flange

NADS[13] and RTNADs[14] distributed around the chamber were added. As the yield increased neutron hardened higher speed versions of the x-ray imaging diagnostic hGXI & DIXI respectively were added.

Figure 3 is a cartoon of the ignition diagnostics and Table 2 gives the acronyms for most of them. An overview of the diagnostic work up to ~ 2015 is given by Kilkenny[5]. Most of the NIF diagnostics development work including hundreds of papers, is recorded in the biannual volumes of the Review of Scientific Instruments (RSI) dedicated to the High Temperature Plasma Diagnostic Conference. Many of these are referenced in a special collection of fourteen invited HED diagnostic review papers[15] in RSI in 2023 and early 2014.

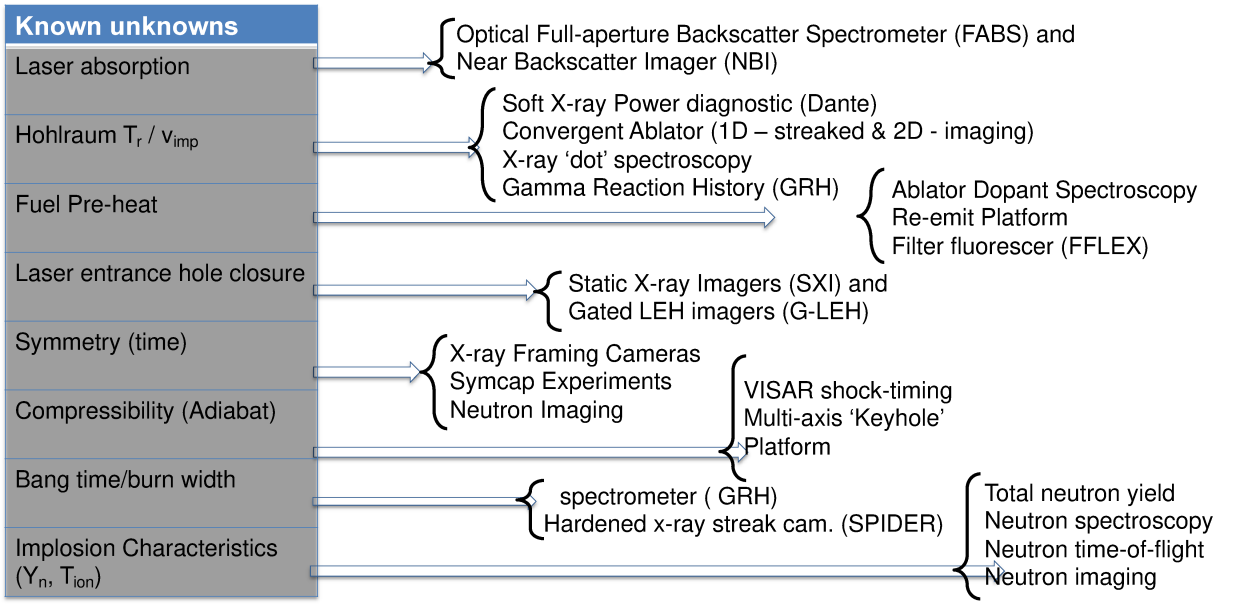

Table 1: The functions of most of the core ignition diagnostics on NIF

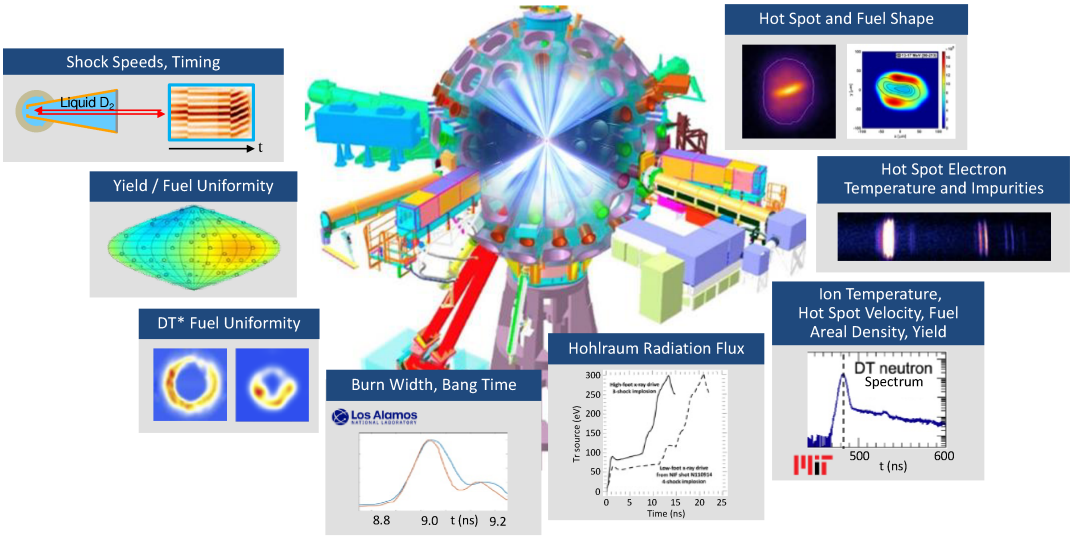

Fig 3. Achieving ignition required many diagnostics to probe the optical, x-ray and nuclear performance of a wide range of ICF implosions and other physics measurements as shown here.

Acronym	Meaning
ARIANE	Active Readout in a Neutron Environment
CNXI	Combined Neutron and X-ray Imager
Dante	Broad-band, time-resolved x-ray spectrometer
dHIRES	DIM HIgh RESolution Spectrometer)
DISC	DIM Insertable (x-ray) Streak Camera
DIXI	Dilation X-ray Imager
DSR	Down Scatter Ratio
FABS	Full Aperture Backscatter Station
FFLEX	Filter Fluorescer
Flange-NADS	Flange Neutron Activation Diagnostic
GLEH	Gated Laser Entrance Hole x-ray pinhole imager
GRH	Gamma Reaction History
GXD	Time-Gated X-ray Detector
hDISC	Hardened DIM Insertable (x-ray) Streak Camera
hGXI	Hardened (gated) X-ray Imager
hSLOS	Hardened SLOS
LEH	Laser Entrance Hole
MRS	Magnetic Recoil Spectrometer

NAD Well-Zr	Neutron Activation Detector in a well using zirconium
NAD–Cu	Neutron Activation Detector using copper
NBI	Near Backscatter Imager
NIS	Neutron Imaging System
pDIXI	Polar Dilation X-ray Imager
RTNADS	Real Time Neutron Activation Detectors
SPBT	South Pole Bang Time
SPIDER	Streaked Polar Instrumentation for Detection of Energetic Radiation
VISAR	Velocity Interferometer System for Any Reflector

Table 2. The NIF core diagnostics and their acronyms

4. Measurements of the conversion of laser light to radiation drive in hohlraums

An early example of how experimental measurements led to the falsification of theory in ICF is described by Nuckolls[16]. X-ray driven ICF using heating of a hohlraum with a 1 μm infrared laser system had been chosen as the research direction by LLNL in the 1970's. Nuckolls said "In high density experiments conducted with Shiva in the late seventies, we crashed into a disastrous plasma physics barrier. We were surprised when disastrous numbers of super-thermal electrons were generated by intense laser light focused into the small hohlraum. 'Hot' electrons penetrated and heated the fusion capsule, so that compression to high densities was not possible. Plasma instabilities also reflected light out of the hohlraum. Fortunately, we had developed state-of-the-art capabilities[17] to diagnose and understand what was happening and to rapidly fabricate improved target designs. We increased the size of the hohlraums and changed the temporal pulse shape and laser focusing in the hohlraum to weaken the plasma instabilities and reduce preheat relative to the ablation pressures. Implosion to one hundred times liquid density was then achieved." Ultimately, the principal change from this falsification was that plans for Nova (the next laser), and then for NIF, were modified to provide an ultra-violet 0.35μ laser.

Nova diagnostics of the conversion of ultra-violet laser energy in ¼ NIF scale hohlraums to x-ray drive put some fundamental uncertainties to rest. Initial ignition designs in the eighties relied on larger lasers than NIF with T_{rad} ~ 200 eV. Ignition designs evolved to smaller hohlraums for NIF requiring hohlraum temperatures ~ 300eV. Many argued that 300 eV was unachievable. Experiments on Nova[18] falsified the objection that these higher temperatures were unachievable. Measurement of laser absorption was approximate at the time with indications that it was close to 100%. Measurements of the x-ray temperature T_{rad} with Dante, a time resolving x-ray band spectrometer, demonstrated T_{rad} up to ~300 eV in agreement with theory as shown in Figure 4. Experiments using shaped radiation pulses were also successfully modeled. Fast electrons were low, typically less than a few percent, indicating super-thermal electron preheat was low. This was excellent validation, albeit approximate, for modeling of laser absorption and hohlraum

albedo. Experiments on OMEGA[19] corroborated this conclusion. As the aforementioned 70's experiments demonstrated, it did not have to be like this.

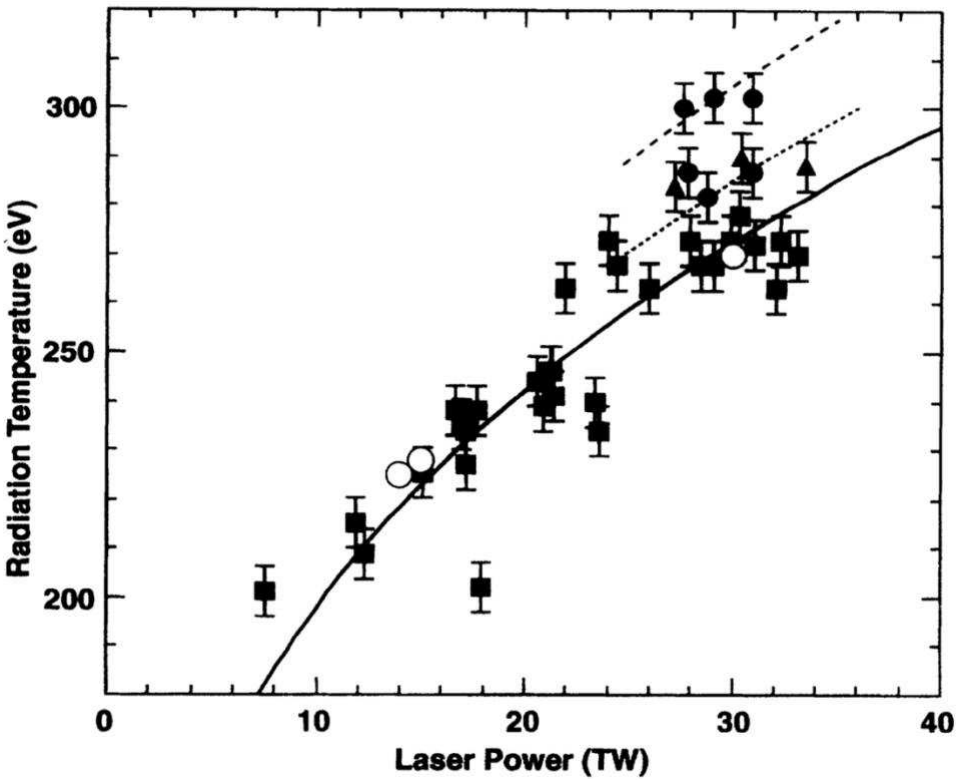

Fig 4 Nova radiation drive scaling from figure 3 of reference [18] with permission.

The first laser absorption and x-ray drive measurements on NIF were equally promising[20]. Initial NIF hohlraums were gas filled with a thin laser entrance hole (LEH) window. The laser absorption versus backscatter such as Stimulated Raman Scattering in NIF hohlraums had been a hotly debated national issue and critics would say an unknown unknown. Laser coupling efficiency was measured from the difference of the incident energy and the backscattered energy into the lens with full aperture backscatter diagnostic station (FABS) and close to the lens with a near (lens) backscatter instrument (NBI) as seen in Fig. 5[21].

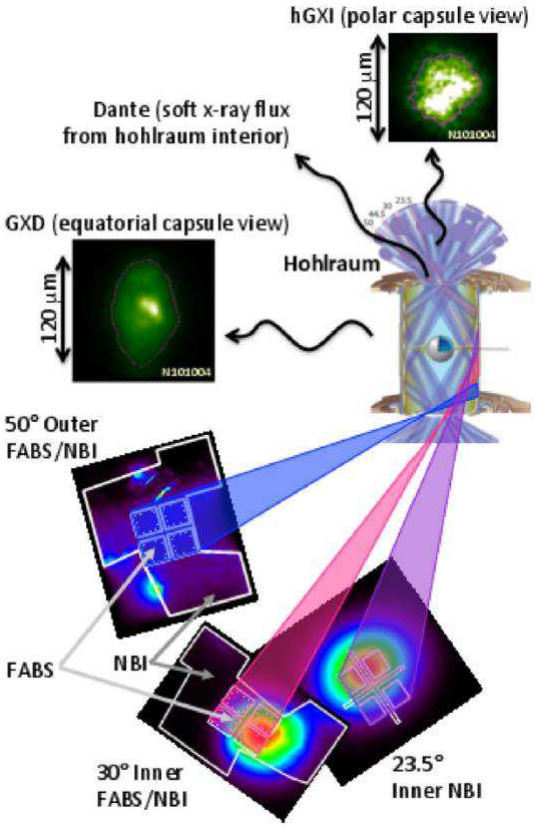

Fig 5 from reference [21] with permission. The hohlraum target is shown in context with optical and x-ray instruments. Backscattered optical light is measured with a FABS and NBI detector on 3 quads. X-rays emitted from the hot spot are measured with equatorial and polar framing cameras. X-ray emission from the interior of the hohlraum is measured using Dante and imaged using SXI.

The initial NIF hohlraum experiments with 1.2 MJ at 0.35 µm showed encouragingly high, 85% to 91% laser coupling. Losses were due to SRS from the laser beams closest to the hohlraum axis that interacted with the dense capsule blow-off plasma. In addition, the experiments indicated a population of hot (> 170 keV) electrons but at acceptable levels, with <0.1% of the total laser energy. Measuring that the hohlraum absorption was close to values assumed in ignition simulations was very important as the radiation drive flows down from the laser absorption. Likewise, it was important to measure an acceptable level of SRS and associated fast electrons, and low enough stimulated Brillouin backscatter to not damage the laser. Later epochs with HDC ablators in section 6 have even higher laser absorption.

The NIF hohlraum radiation field is sampled by two absolutely calibrated x-ray spectrometers (Dantes), imaging the size of the LEH (SXI), and an absolutely calibrated hard x-ray spectrometer FFLEX (Table1). Initial experiments on NIF[20] demonstrated a 300eV shaped pulse in ignition scale cryogenic gas filled targets. The ability to achieve 300 eV in a NIF ignition hohlraum had been questioned by some, so these measurements were encouraging. Again, as Nuckolls discovered it did not have to be like this.

5. Diagnostic Platforms for NIC and the high foot epochs

The first epoch of NIF from 2009 to about 2013 was called the National Ignition Campaign (NIC). Experiments followed the point design[3] in an attempt to achieve ignition. The ignition core diagnostics were used in a variety of experimental arrangement called platforms to measure and control the four high level variables: shape, adiabat, velocity and mix. This was followed by a high foot epoch, also using plastic ablators.

5a: Shape

The >30 fold radial convergence required for NIF ignition requires precise control of the capsule implosion. Since the late 80s it been recognized that the fundamental asymmetry for the x-ray drive was a long wavelength pole to waist (P_2 Legendre polynomial) radiation flux variation. Nova experiments[22] confirmed that the long wavelength mode dominated and can be systematically varied from shot to shot by changing the beam pointing in a hohlraum whose length was varied. The capsules were plastic ablators filled with gas to provide x-ray emission at stagnation. The shape of the emission was observed with time resolved (~100 psec) x-ray imaging using a GXD as well as time integrated x-ray imagers. In these experiments and virtually all experiments to date, the imager was an array of pinholes and the platform was called a symcap, for symmetry capsule. A code was used to predict the laser pointing to get a round stagnation image of the implosion. The data usually did not quite agree with simulations; that is the micro-falsification of fig 1, so a target and laser on Nova or laser on NIF adjustment was made to get round image on the next shot. This technique which uses so called Symcap targets is one of the four tuning legs that is used to tune symmetry.

NIF uses cryogenic gas filled capsules as ignition surrogates or Symcaps to adjust experimental conditions such as the hohlraum length, beam cone balance and cone wavelength difference needed for a symmetric implosion. To measure the time integrated symmetry, a neutron-hardened time-gated or time-integrated x-ray imager hGXI and a neutron imager were used on a symcap, providing micro-falsification of the simulations. Importantly the image being either oblate or prolate shows which way to make a symmetry adjustment with cross beam energy transfer (CBET)[23] on the next shot. A wavelength shift of up to 0.9 nm between the inner and outer cones of beams provided control of the P_2 asymmetry[3, 20]. The shape of the subsequent layered implosion is loosely correlated to tuning the symcap. As suggested by the NAS this is a known unknown because the model is not precise enough to meet the very demanding symmetry requirement of ignition. This technique was able to control the symmetry of the assembly phase of the implosion of the surrogate implosions to several % in core shape P_2. This is a good example of micro-validation. CBET was predicted to be the dominant lever on P_2 and the first NIF shot validated this.

For ignition, drive symmetry must be maintained throughout the complex laser pulse not just at the end. Re-emit capsules were used to measure the symmetry early in the pulse[24, 25]. In these targets, a sphere of Bi replaced the plastic ignition capsule. A high atomic number is used because of the high albedo for the radiation incident on the surface. Re-emitted x-rays in proportion to the incident flux were measured by a GXD. This re-emission is used to measure and set the low mode polar and azimuthal radiation flux asymmetry during the first 2 ns of the pulse. This is another example of micro-falsification where imaging shows which way to make a correction in beam balance at the beginning of the NIF ignition pulse.

5b:Adiabat

Another of the NAS known unknowns is the shock timing, related to the adiabat. Shock timing with VISAR was developed on OMEGA and Nova, a novel use leading to a platform to measure the shock timing in an ignition surrogate capsule[26, 27]. The initial concept was to time the shocks in a planar sample attached to the side of the hohlraum[28]. This evolved to measuring the shocks inside a capsule, in a re-entrant "keyhole" platform as shown in Figure 6. VISAR is an interesting example of a diagnostic that was initially developed for equation-of-state experiments, yet later became a core ICF diagnostic on NIF. For ignition it is used to time the sequence of ablatively driven shocks in an ignition surrogate implosion. This configuration was beautifully shown to determine the fuel adiabat as shown in Figure. 7. The single view "keyhole" target evolved to a platform measuring the shock breakout in perpendicular directions inside the surrogate capsule with the use of a small turning mirror[29]. This gave 2-axis shock timing data, another measure of radiation asymmetry at a later time than re-emit platforms. An enclosed VISAR turning mirror in a keyhole surrogate platform is now used routinely before ignition implosions. Micro-falsification from shock timing measurements on a surrogate target guides a small change in the laser pulse shape to attain desired adiabat of the fuel as well as pole waist shock breakout symmetry. Two of the NAS known unknowns from one platform!

Diagnostic configuration

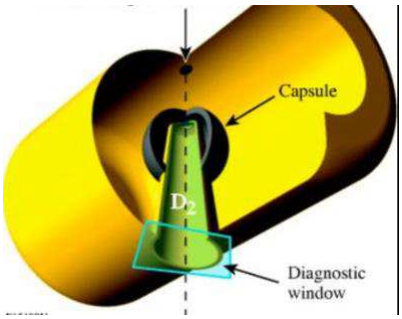

Boehly, Munro et al, *Phys. Plasmas* **16** 056302 (2009)

Fig 6 from reference 26 with permission.

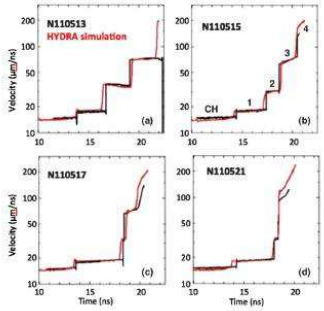

Robey et al, PRL **108** 215004 (2012)

Fig 7 from reference 27 with permission.
Additionally, VISAR discovered an arguably unknown unknown: frost on the laser entrance window (Celliers, private communication, 2013). Early VISAR timing shots[30] revealed a significant discrepancy between the observed shock velocity history and pre-shot predictions based on simulations. The shock arrival at the CH-D_2 interface was found to be several ns later than theory, and its velocity too high and close to the second shock level. The leading hypothesis to explain this result was that residual chamber gases (N_2, O_2, H_2O etc,) had condensed on the laser entrance hole (LEH) windows to form ice layers of the order of 1–2 μm thick. This ice layer impeded the initial heating of the hohlraum such that the first shock was weak and travelled so slowly that the second shock merged with it in the CH ablator prior to its emergence into the liquid D_2. A target modification to mitigate the LEH-ice problem was implemented: it consisted of a thermally isolated membrane (called a "storm window") placed 500 μm away from the LEH window to provide a membrane heated slightly by ambient infrared thus preventing the chamber gases from condensing on the cold LEH-window[31]. Interestingly although the ice was a surprise on the first timing shots the effect had been previously experimentally tested in the NIF target chamber years before and was thought to be insignificant;: a known, incorrectly measured known.

5c. Implosion velocity

The third leg is the implosion velocity, measured by backlighting a surrogate low yield implosion, either a Symcap or a low yield implosion; the platform is called a ConA, short for convergent ablator. Radiography typically uses 8-10keV x-rays, to measure the radius of the imploding shell versus time and the optical depth of the remaining ablator areal density as it implodes with a framed imager or a streak camera[4, 32]. Initially a GXD was used as a detector and then when available an x-ray streak camera; neither is hard enough to use on a high yield shot. This measurement of a known unknown is used to adjust the laser peak power and the shell thickness so that the implosion has both the required velocity and the required residual mass of ablator. The peak power and shell thickness along with the dopant level in the ablator must be adjusted to optimize the tradeoff between implosion velocity and mix.

5d. Mix

The fourth leg is the amount of mix of higher Z ablator into the core, radiating and cooling it. Structured x-ray brightness assumed due to heterogeneous mixing of ablator material and fuel into the hot spot[33] using a GXD was an early observable. In addition special targets with tracer mid-Z dopants produced spectroscopic signatures to measure mix, using an x-ray spectrometer[34] and then a set of hardened x-ray spectrometers[6] . Heterogeneous mix was arguably an unknown unknown.

The mix mass was also inferred[35] from the excess of bremsstrahlung and free-bound emission from the compressed hotspot relative to that expected for emission from clean DT. The diagnostic was an absolutely calibrated pinhole imager and sets of Ross pair filters measuring the core emission. Strong performance degradation was seen at levels of several hundred nanograms of mix mass, consistent with expected sensitivity to the mix.

Landen[36] describes a series of shots varying a parameter to validate theory. A vivid example of trend analysis was made by Ma[35] in Fig. 8. Implosion velocity in a series of DT layered

implosions was varied by changing the ablator thickness. The amount of ablator mixing into the hot x-ray emitting core was measured by absolutely calibrated x-ray diagnostics as seen in Figure 8.

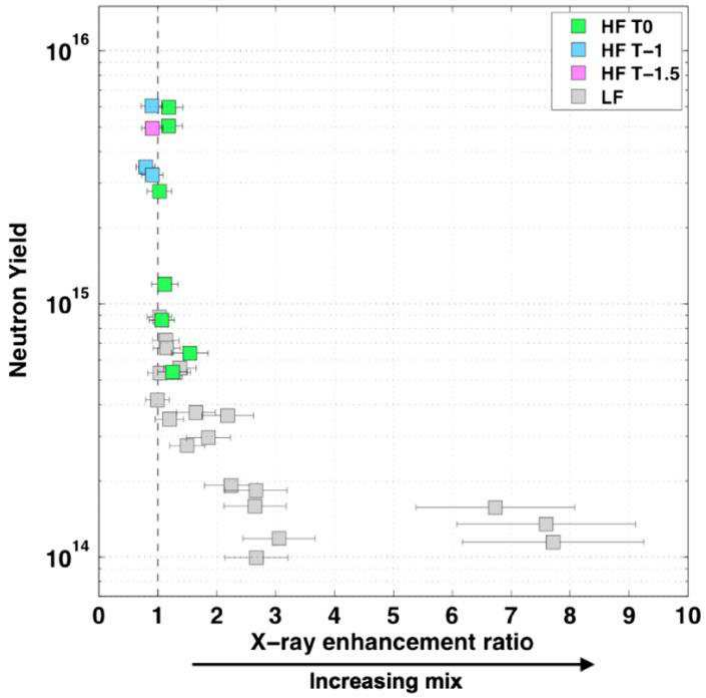

Fig 8 from Ma reference [35] with permission. DT neutron yield ve x-ray enhancement ratio for the cryogenic DT implosions completed on the NIF. "HF" refers to high-foot implosions; "LF" refers to low-foot implosions. The thinner shell implosions continue to cluster around the zero mix region

The trend shown in Figure 8 qualitatively validated theory about implosion performance degradation as instability gets worse with higher velocity implosions. It is difficult to replicate the observed levels of mix in the simulations. Mix had always been known as a limiting factor for ignition that was difficult to calculate: a known unknown.

5e. High foot implosions and hydro growth radiography (HGR)

The completion of the NIC was followed by series of experiments using a higher foot in the laser pulse at early time, resulting in a lower instability phase and an expansion in the number of experimental platforms and designs used by the ICF program. The high foot design is predicted to reduce the growth of hydrodynamic instabilities at the ablation front by increasing the fuel adiabat from 1.5 to 2.7. A side effect is the limitation of the maximum achievable areal density, although adiabat shaping techniques[37]were shown to partially mitigate this. Direct measurements of the hydrodynamic growth were made using the hydro growth radiography (HGR) platform; this was a good example of micro-validation of theory.

The HGR platform used an x-ray gating camera to directly measure the growth of pre-imposed perturbations at the ablation front of a surrogate fusion capsule as shown in Figure 9 .

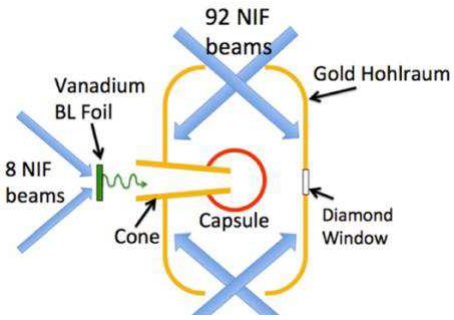

Fig 9 from Raman, reference [38] with permission.

A backlighter foil is used to project x-rays through a surrogate capsule in the 'keyhole' configuration onto a gated x-ray framing camera. Ripples of known amplitude and spatial frequency are machined onto the capsule surface. The single-mode growth of these ripples is measured in transmission and compared with radiation hydrodynamic simulations. Figure 10[38] compares the simulated and measured growth factors for the high-foot and low-foot designs. These data show that the ablation front growth is reduced for the high foot design validating theory.

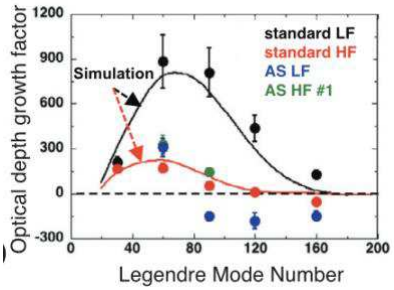

Fig 10 from Raman reference [38] with permission.

There is also an unknown, unknown way to look at this result. It suggests that the failure to anticipate ablator mix into the hotspot during the NIC was due to incomplete understanding of the perturbation seeds from target imperfections rather than inaccurate calculations of ablation front Rayleigh Taylor growth; the initial conditions of the implosion targets was not known precisely enough.

The initial ignition campaign on NIF with plastic ablators focused on demonstrating control of the hohlraum drive and then the key theoretical observable of implosions using a low foot 4-step laser pulse. Laser absorption and radiation temperatures were close to expectations. Control of

the shape, adiabat, velocity and mix parameters was demonstrated. None of these parameters were known precisely enough beforehand and were tuned in by the core diagnostics. Additionally, the diagnostics revealed some unknown, or maybe forgotten unknowns such as ice on the LEH window and structured emission from ablator mix into the hot spot.

However, the thermonuclear yields of these implosions were 3-10 times lower than expected. The diagnostics were mainly pass /fail, hinting at issues by doing trend analysis[36]. X-ray imaging hinted at fill tube and support tent perturbation issues. X-ray measurements gave a crude mix mass in excess of expectation. Angular measurements of down-scattered neutrons indicate that there could be low spatial mode asymmetries in the compressed main fuel, which may explain some of the deficit in pressure and the larger than expected mix.

6 Role of diagnostics in the post NIC /high foot epochs leading up to ignition

This is a diagnostic paper and so only a very brief discussion of experimental activities is appropriate here. The early experimental work, section 5, developed the foundational platforms, diagnostics, and knowledge required to achieve ignition. Many critical experimental capabilities developed during this phase used plastic ablators. This epoch was followed by a high density carbon (HDC) ablator epoch[39]. Development of a high density carbon (HDC) ablator material, low gas fill hohlraums and symmetry control were critical to achieving ignition. The use of thin (70 μm) HDC ablators enabled shorter laser pulses, hence lower gas-fill hohlraums, less LPI losses and better control of x-ray drive asymmetries[40, 41].

The ~3X increase in density of HDC vs. CH allowed for ~2X thinner capsule and ~2X shorter laser pulse. Shorter HDC laser pulses allowed for hohlraum gas density to be reduced, bypassing ~200 kJ of laser backscatter. The shorter laser pulse and higher coupling efficiency allowed for improved symmetry tuning and higher yields[41-43]. The HDC experiments controlled low mode asymmetry throughout the laser history, achieving increased fusion yield[40] (54 kJ). The implosion symmetry is controlled throughout the laser drive history by adjusting the relative power balance between the inner and outer laser cones. Improved symmetry and drive, although measured with surrogate targets, helped to enable the first burning plasma with alpha heating becoming the dominant heating source. After the burning plasma experiments, significant improvements to the capsule quality were made. Increased hohlraum efficiency and laser energy with improved targets all directly contributed to achieving ignition.

During this time, diagnostic advances were informing our understanding of the origin and impact of asymmetries and mix. Degradation from an asymmetry in compression from laser, target and capsule sources was identified and quantified. This improved symmetry, and the identification of sources of localized mix from fill tube and capsule perturbations, led to improved fusion performance quantified as shown in Figure 11.

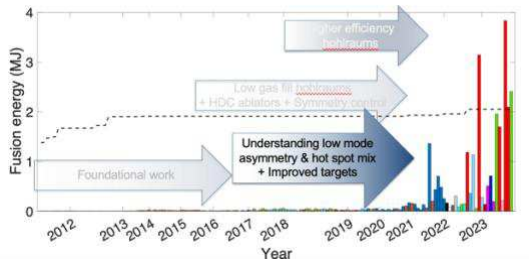

Figure 11 The epochs of ignition on NIF

6a Shape again

Symmetry at earlier times during an implosion was a missing aspect of the measurements. This was partially addressed by the new 2D Convergent Ablator (2D ConA) back-lit radiography platform. A schematic of the experimental arrangement is shown in Figure 12, from Rygg[44]. This platform used the existing GXDs, which restricted the platform to low n yield surrogate implosions.

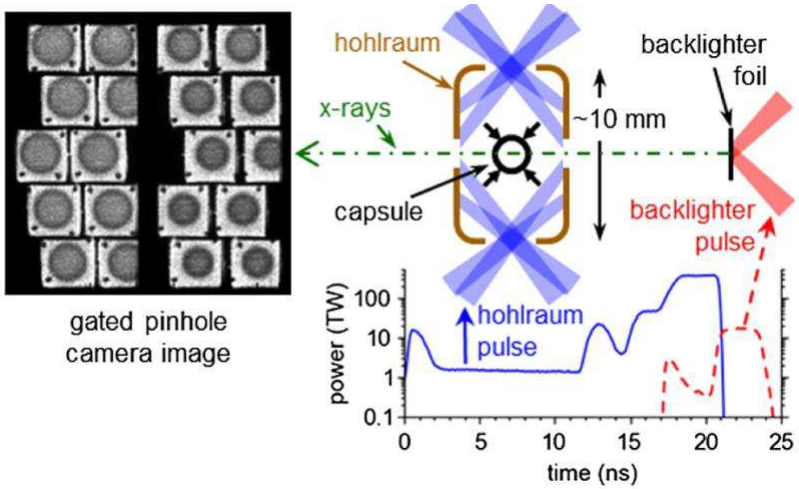

Fig 12 from reference 44 with permission.

Measurements of the ablator shell shape at peak velocity showed a substantial four-fold asymmetry that was not observed in the hot spot emission showing that the implosion symmetry inferred from x-ray self-emission of the hot spot was not representative of drive asymmetry at earlier times. Arguably an unknown, unknown.

Up to this day a 2D ConA experiment is usually done before a high yield layered implosion on a surrogate gas filled target allowing experimentalists to check their tuning of the symmetry on a less expensive target. 2D ConA cannot be used on high yield layered implosion because (1) some of the drive beams would be needed for backlighting changing the symmetry and (2) there would be too much neutron induced background on today's gated x-ray imagers. Work on this known unknown continues to this day; polar symmetry swings are probably a significant remaining yield degradation mechanism.

6b Tent scar

In addition, the 2D ConA platform revealed a major undermodeled drive asymmetry issue. The capsule is supported in the hohlraum by a thin (<300 nm) plastic tent as shown in fig 13 . Backlit images revealed a large perturbation in the shell optical density (and therefore ρR) where the capsule support tent lifts off the capsule, as seen in Fig. 14. The magnitude of the 'tent scar' was far larger than initially expected. At the start of the NIC campaign we had estimates for the effect of the capsule support but full simulations could not yet be not done. Modeling missed essential physics—the velocity/momentum impact of the exploding tent. This was a known but badly underestimated unknown until revealed by experiment.

Figure 14 compares the tent scar[45] for the NIC low-foot design and the high foot design showing the lower growth as expected for the high foot. High foot designs were used for most subsequent ignition attempts and the tent thickness was also decreased. On early NIF shots, the tent membrane was 300 nm thick; as technology improved, targets were built with 110 nm, 45 nm, 30 nm, and as thin as 12 nm tents.

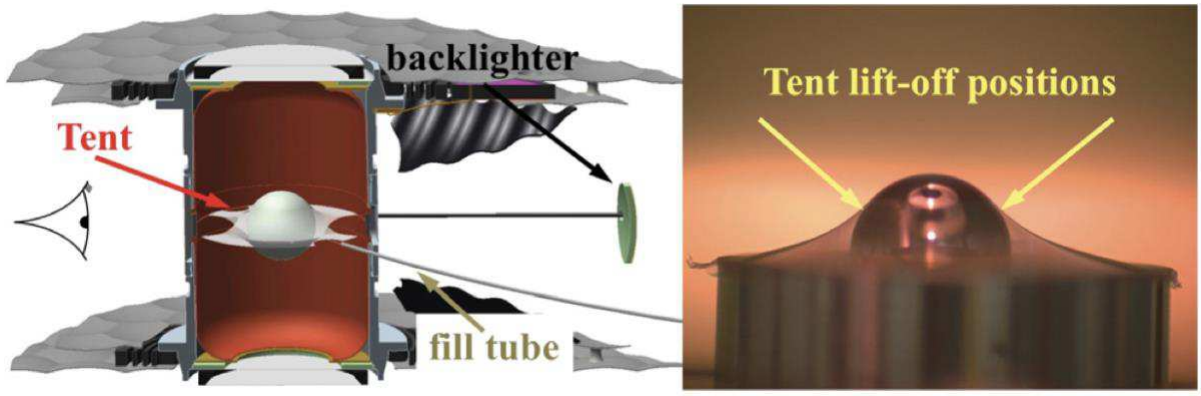

Fig 13 from reference 45 with permission

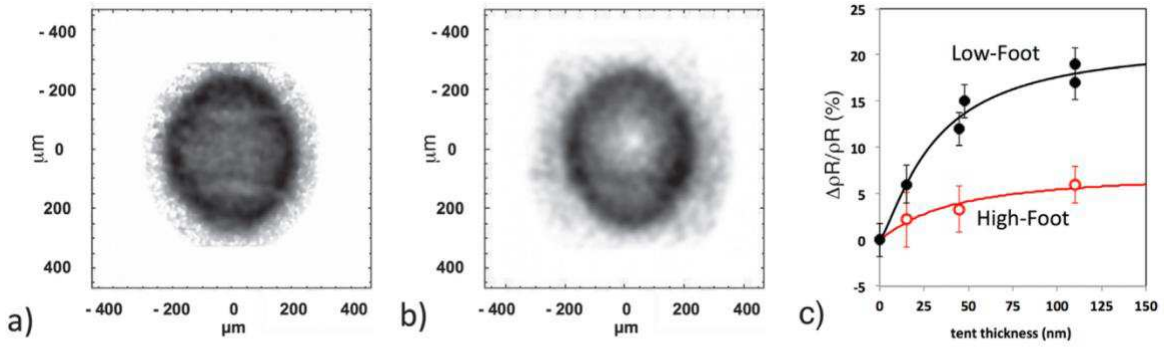

Figure 2. Comparison of radiographs of implosions driven by (a) low-foot and (b) high-foot laser pulses using 47 nm and 45 nm tents, respectively. (c) The fractional variation in ρR increases with tent thickness and is $\approx 3\times$ larger for the low-foot pulse than for the high-foot pulse. Reproduced with permission from Tommasini *et al* [20].

Figure 14. From reference [46] with permission.

6c. Fill tube induced mix.

Another vivid example of x-ray imaging showing a capsule technology feature degrading performance is the capsule fill tube. For ignition capsule designs, the ablators are relatively impermeable and need a fill tube. Initial simulations were not precise enough and indicated that a 10 μm fill tube was tiny enough to avoid significant perturbations and mix. However x-ray imaging of both plastic and high density carbon ablators usually shows a spot of x-rays identifiable with the position of the fill tube[47-49]. Current ignition capsules seem to need a maximum of 2 micron fill tube diameter. This is a known but underestimated unknown.

The neutron imager also images hard x-rays in the CNXI configuration. The CNXI covers the existing neutron penumbral apertures with x-ray pinholes. The thin high-Z foil used for the x-ray pinholes does not affect the neutron imaging performance of the system, and the thick neutron imaging aperture does not obstruct the x-ray images as long as the source is in the clear-aperture field of view of the penumbra. A passive detector installed along the line of sight, inside the vacuum chamber, records x-ray images but again has minimal effect on the transmission of neutrons through to the neutron imaging system downstream. Time integrated x-ray and neutron emission can be overlaid[50] as in Figure 15 showing a decrease in neutron emission correlating spatially with cooling by entrained carbon ablator from the fill tube region flowing into the hot core.

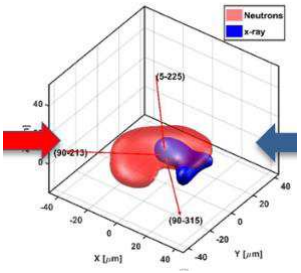

Fig 15 from P Volegov reference [50] with permission

6d Ablator surface imperfections

There is a similar story about the effects of divots and high-Z impurities in the ablator. The effect of divots was calculated but underestimated. For the HDC capsules in particular many spots of x-ray emission are seen in the compressed core[51]. Recently higher quality HDC targets with fewer divots do seem to produce less localized x-ray emission and a highr neutron performance. This issue is like the fill tube issue. Efforts were initially made to calculate the detriment effect on performance but the accuracy remains insufficient.

6e Azimuthal asymmetry

The nToFs on NIF were developed over a decade and half by LLE and LLNL, eventually achieving incredible energy resolution[52]. Placed at several locations around the chamber they can measure the flow velocity of the burning hot spot from the differences in arrival times[53]. Drift velocities of the burning plasma up to 100 km/s were initially observed. Like the imaging diagnostics, the array of nToFs does identify a direction of asymmetries of drive or ablator anisotropy on a particular shot. Asymmetries were identified by trending from laser imbalances, capsule thickness nonuniformity, and drive losses through necessary apertures in the hohlraum[54-56]. The nToF measurement drove an increased scrutiny on the initial concentricity of the ablator[57]. The nonzero hot-spot velocity can cause a significant yield degration and was an unanticipated or at least under estimated unknown. The diagnostic measurement caused the geometry of the x-ray observation window in the hohlraum and the concentricity of the ablator to be improved. Arguably an unknown unknown.

7 Diagnostic Signatures of Ignition

Signatures of the onset of burn and ignition are seen across several types of measurements. The increased fusion neutron yield was measured by three independent, absolutely calibrated diagnostics: Zr and Cu activation (NADs) and the Magnetic Recoil Spectrometer (MRS) agreeing within several %. The ion temperature from the width of the un-scattered primary increased significantly from 5-6 keV to greater than 10 KeV

The radius of the x-ray emission from the remaining ablator increases as the alpha energy from the ignition explodes the x-ray emission[58] as shown in Figure 16.

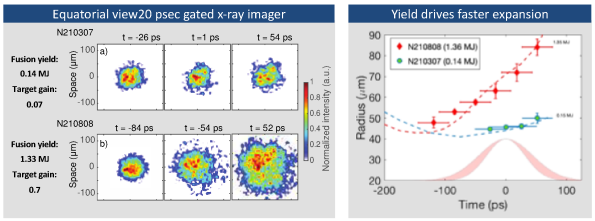

Figure 16 from reference 58 with permission.

Further evidence of significant burn is that burn durations decreased to less than 100ps, from disassembly driven by the high pressure of the burning fuel. Simulations have previously indicated that while the overall duration during which fusion reactions occur increases when the plasma ignites, the duration during which the majority of the fusions occur decreases, leading to a sharper peak, and smaller full-width at half maximum burn duration.

An overlooked signature of high yield corroborating the other yield diagnostics came from the Dante time resolving x-ray spectrometer, measuring the temperature in the hohlraum. Figure 17 shows the signal measured by the Dante diagnostic as the ignition threshold is reached[59]. As well as the normal peak from the laser heating there is a second sharp peak that correlates in time with shortly after the capsule bang-time. This is due to the alpha particle heating of the remaining high Z of the capsule ablator which radiates and reheats the hohlraum after the laser turns off at about 8 ns in the figure. This feature is apparently routinely seen in integrated (hohlraum and

capsule) calculations of igniting designs but that was unknown to most scientists working in the field. A forgotten unknown.

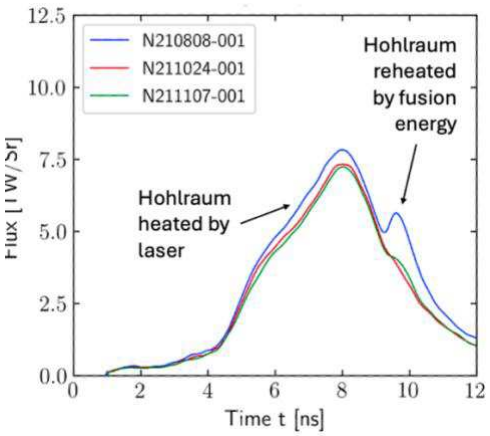

Figure 17 from reference 59 with permission.

7 Summary

Achieving ignition on NIF has required different types of experiments with a core set of diagnostics, some quantifying known unknowns, and some revealing surprises, arguably unknown unknowns. Early design work realized that the extreme precision required for ignition on NIF would require fine tuning by experiment, measuring and adjusting known unknowns. Many examples are given where the use of a core set of ignition diagnostics in experimental arrangements called platforms, demonstrated control of the key theoretical parameters shape, adiabat, velocity and mix. The discovery of the direction of adjustments needed is either by trend analysis or in many cases seeing from the diagnostic which way to make an adjustment. But in addition, experimental platforms have revealed some unknown factors degrading performance that were unknown unknowns. Some of these factors had been previously thought of but underestimated. The total methodology is a variant of Popper's falsifiability philosophy of science.

AUTHOR DECLARATIONS

The authors have no conflicts of interest to disclose.

AUTHOR CONTRIBUTIONS

J. D. Kilkenny: Conceptualization (equal); lead author: S. Batha: Section neutron imaging:W. W. Hsing: references. M. Gatu-Johnson:nuclear data: J. Mackinnon conceptualization: S. P. Regan conceptualization: A. Pak input experimental results: O L Landen conceptualization: A. S. Moore nuclear data: N. B. Meezan conceptualization: S. W. Haan conceptualization: D. K. Bradley conceptualization.

References

1. Indirect Drive ICF Collaboration, Phys. Rev. Lett. **129** (7), 075001 (2022).
2. K. Popper, *The Logic of Scientific Discovery*. (Hutchinson, 1974).
3. J. D. Lindl, O. L. Landen, J. Edwards, E. I. Moses, J. Adams, P. A. Amendt, N. Antipa, P. A. Arnold, L. J. Atherton, S. Azevedo, D. Barker, M. A. Barrios, I. Bass, S. H. Baxamusa, R. Beeler, B. V. Beeman, P. M. Bell, L. R. Benedetti, L. Bernstein, L. B. Hopkins, S. D. Bhandarkar, T. Biesiada, R. M. Bionta, D. L. Bleuel, E. J. Bond, M. Borden, M. W. Bowers, D. K. Bradley, D. Browning, G. K. Brunton, J. Bude, S. C. Burkhart, R. F. Burr, B. Butlin, J. A. Caggiano, D. A. Callahan, A. C. Carpenter, C. W. Carr, D. T. Casey, C. Castro, J. Celeste, P. M. Celliers, C. J. Cerjan, J. Chang, M. Chiarappa-Zucca, C. Choate, T. J. Clancy, D. S. Clark, S. J. Cohen, G. W. Collins, A. Conder, J. R. Cox, P. S. Datte, G. A. Deis, E. L. Dewald, P. Di Nicola, J. M. Di Nicola, L. Divol, S. N. Dixit, T. Döppner, V. Draggoo, O. Drury, R. Dylla-Spears, E. G. Dzenitis, J. M. Dzenitis, M. J. Eckart, D. C. Eder, J. H. Eggert, R. B. Ehrlich, G. V. Erbert, J. Fair, D. R. Farley, M. Fedorov, B. Felker, R. Finucane, A. Fisher, D. N. Fittinghoff, J. Folta, R. J. Fortner, T. Frazier, G. Frieders, S. Frieders, S. Friedrich, J. Fry, J. Gaylord, S. M. Glenn, S. H. Glenzer, B. Golick, G. Gururangan, G. Guss, S. W. Haan, B. J. Haid, B. Hammel, A. V. Hamza, E. P. Hartouni, R. Hatarik, B. W. Hatch, S. P. Hatchett, R. Hawley, C. Haynam, J. Heebner, G. Heestand, M. R. Hermann, V. J. Hernandez, D. G. Hicks, D. E. Hinkel, D. D. Ho, J. P. Holder, D. Holunga, J. Honig, J. Horner, R. K. House, M. Hutton, N. Izumi, M. C. Jackson, K. S. Jancaitis, D. R. Jedlovec, M. A. Johnson, O. S. Jones, D. H. Kalantar, R. L. Kauffman, L. Kegelmeyer, G. Kerbel, M. Key, S. F. Khan, J. R. Kimbrough, R. Kirkwood, J. J. Klingman, J. A. Koch, T. R. Kohut, J. M. Koning, K. M. Knittel, B. J. Kozioziemski, G. W. Krauter, K. Krauter, A. Kritcher, J. Kroll, W. L. Kruer, G. LaCaille, K. N. LaFortune, L. J. Lagin, T. A. Land, A. B. Langdon, S. H. Langer, D. W. Larson, D. A. Latray, T. Laurence, S. LePape, R. A. Lerche, Z. Liao, J. Liebman, R. A. London, R. R. Lowe-Webb, T. Ma, B. J. MacGowan, A. J. MacKinnon, A. G. MacPhee, T. N. Malsbury, K. Manes, A. M. Manuel, E. R. Mapoles, M. M. Marinak, C. D. Marshall, D. Mason, N. Masters, D. G. Mathisen, I. Matthews, T. McCarville, J. M. McNaney, D. J. Meeker, N. B. Meezan, J. Menapace, P. Michel, P. E. Miller, J. L. Milovich, M. Mintz, R. Montesanti, M. Monticelli, J. D. Moody, M. J. Moran, J. C. Moreno, D. H. Munro, R. A. Negres, J. R. Nelson, M. Norton, M. Nostrand, M. O'Brien, Y. P. Opachich, C. Orth, A. E. Pak, E. S. Palma, J. N. E. Palmer, T. G. Parham, H. S. Park, P. K. Patel, R. W. Patterson, J. E. Peterson, J. L. Peterson, T. Phillips, R. Prasad, K. Primdahl, S. T. Prisbrey, S. R. Qiu, J. E. Ralph, K. S. Raman, F. Ravizza, B. Raymond, B. A. Remington, M. A. Rever, J. Reynolds, M. J. Richardson, A. C. Riddle, B. Rittmann, M. D. Rosen, J. S. Ross, J. R. Rygg, R. A. Sacks, J. T. Salmon, J. D. Salmonson, J. D. Sater, R. L. Saunders, R. Sawicki, K. Schaffers, D. H. Schneider, M. B. Schneider, H. A. Scott, S. M. Sepke, R. Seugling, D. A. Shaughnessy, M. J. Shaw, R. Shelton, N. Shen, N. Shingleton, N. Simanovskaia, V. Smalyuk, D. A. Smauley, M. Spaeth, B. K. Spears, D. R. Speck, T. M. Spinka, P. T. Springer, M. Stadermann, W. Stoeffl, J. Stolken, C. Stolz, E. Storm, D. J. Strozzi, T. Suratwala, L. J. Suter, J. S. Taylor, C. A. Thomas, G. L. Tietbohl, R. Tommasini, D. Trummer, B. VanWonterghem, R. Von Rotz, R. J. Wallace, C. F. Walters, A. Wang, A. L. Warrick, S. Weaver, S. V. Weber, P. J. Wegner, K. Widmann, C. C. Widmayer, E. A. Williams, P. K. Whitman, K. Wilhelmsen, M. Witte, L. Wong, R. D. Wood, S. Yang, C. Yeamans, B. K. Young, B. Yoxall, R. A. Zacharias, G. B. Zimmerman, S. Batha, C. R. Danly, V. Fatherley, G. P. Grim, N. Guler, H. W. Herrmann, Y. Kim, J. L. Kline, G. A. Kyrala, R. J. Leeper, D. Martinson, F. E. Merrill, R. E. Olson, C. Wilde, M. D. Wilke, D. C. Wilson, G. A.

Chandler, G. W. Cooper, K. D. Hahn, K. J. Peterson, C. L. Ruiz, K. C. Chen, N. Dorsano, M. Emerich, C. Gibson, D. Hoover, M. Hoppe, J. D. Kilkenny, K. Moreno, H. Wilkens, S. Woods, J. A. Frenje, M. G. Johnson, C. K. Li, R. D. Petrasso, H. Rinderknecht, M. Rosenberg, F. H. Séguin, A. Zylstra, W. Garbett, P. Graham, T. Guymer, A. S. Moore, J. L. Bourgade, P. Gauthier, J. P. Leidinger, L. Masse, F. Philippe and R. H. H. Scott, Phys. Plasmas **21** (12) (2014).

4. O. L. Landen, J. Edwards, S. W. Haan, H. F. Robey, J. Milovich, B. K. Spears, S. V. Weber, D. S. Clark, J. D. Lindl, B. J. MacGowan, E. I. Moses, J. Atherton, P. A. Amendt, T. R. Boehly, D. K. Bradley, D. G. Braun, D. A. Callahan, P. M. Celliers, G. W. Collins, E. L. Dewald, L. Divol, J. A. Frenje, S. H. Glenzer, A. Hamza, B. A. Hammel, D. G. Hicks, N. Hoffman, N. Izumi, O. S. Jones, J. D. Kilkenny, R. K. Kirkwood, J. L. Kline, G. A. Kyrala, M. M. Marinak, N. Meezan, D. D. Meyerhofer, P. Michel, D. H. Munro, R. E. Olson, A. Nikroo, S. P. Regan, L. J. Suter, C. A. Thomas and D. C. Wilson, Phys. Plasmas **18** (5) (2011).

5. J. D. Kilkenny, P. M. Bell, D. K. Bradley, D. L. Bleuel, J. A. Caggiano, E. L. Dewald, W. W. Hsing, D. H. Kalantar, R. L. Kauffman, D. J. Larson, J. D. Moody, D. H. Schneider, M. B. Schneider, D. A. Shaughnessy, R. T. Shelton, W. Stoeffl, K. Widmann, C. B. Yeamans, S. H. Batha, G. P. Grim, H. W. Herrmann, F. E. Merrill, R. J. Leeper, J. A. Oertel, T. C. Sangster, D. H. Edgell, M. Hohenberger, V. Y. Glebov, S. P. Regan, J. A. Frenje, M. Gatu-Johnson, R. D. Petrasso, H. G. Rinderknecht, A. B. Zylstra, G. W. Cooper and C. Ruiz, Fusion Sci. Technol. **69** (1), 420-451 (2016).

6. J. D. Kilkenny, W. W. Hsing, S. H. Batha, G. A. Rochau, T. C. Sangster, P. M. Bell, D. K. Bradley, H. Chen, J. A. Frenje, M. Gatu-Johnson, V. Y. Glebov, R. J. Leeper, A. J. Mackinnon, S. P. Regan, J. S. Ross and J. L. Weaver, Rev. Sci. Instrum. **94** (8) (2023).

7. O. L. Landen, D. T. Casey, J. M. DiNicola, T. Doeppner, E. P. Hartouni, D. E. Hinkel, L. F. B. Hopkins, M. Hohenberger, A. L. Kritcher, S. LePape, B. J. MacGowan, S. Maclaren, K. D. Meaney, M. Millot, P. K. Patel, J. Park, L. A. Pickworth, H. F. Robey, J. S. Ross, S. T. Yang, A. B. Zylstra, K. L. Baker, D. A. Callahan, P. M. Celliers, M. J. Edwards, O. A. Hurricane, J. D. Lindl, J. D. Moody, J. Ralph, V. A. Smalyuk, C. A. Thomas, B. M. Van Wonterghem and C. R. Weber, High Energy Dens. Phys. **36** (2020).

8. J. D. Kilkenny, Rev. Sci. Instrum. **63** (10), 4688-4694 (1992).

9. National Ignition Facility Conceptual Design Report, UCRL-PROP-117093 ES, Lawrence Livermore National Laboratory, 1994.

10. S. W. Haan, S. M. Pollaine, J. D. Lindl, L. J. Suter, R. L. Berger, L. V. Powers, W. E. Alley, P. A. Amendt, J. A. Futterman, W. K. Levedahl, M. D. Rosen, D. P. Rowley, R. A. Sacks, A. I. Shestakov, G. L. Strobel, M. Tabak, S. V. Weber, G. B. Zimmerman, W. J. Krauser, D. C. Wilson, S. V. Coggeshall, D. B. Harris, N. M. Hoffman and B. H. Wilde, Phys. Plasmas **2** (6), 2480-2487 (1995).

11. S. W. Haan, J. D. Lindl, D. A. Callahan, D. S. Clark, J. D. Salmonson, B. A. Hammel, L. J. Atherton, R. C. Cook, M. J. Edwards, S. Glenzer, A. V. Hamza, S. P. Hatchett, M. C. Herrmann, D. E. Hinkel, D. D. Ho, H. Huang, O. S. Jones, J. Kline, G. Kyrala, O. L. Landen, B. J. MacGowan, M. M. Marinak, D. D. Meyerhofer, J. L. Milovich, K. A. Moreno, E. I. Moses, D. H. Munro, A. Nikroo, R. E. Olson, K. Peterson, S. M. Pollaine, J. E. Ralph, H. F. Robey, B. K. Spears, P. T. Springer, L. J. Suter, C. A. Thomas, R. P. Town, R. Vesey, S. V. Weber, H. L. Wilkens and D. C. Wilson, Phys. Plasmas **18** (5) (2011).

12. Committee for the Review of the Department of Energy's Inertial Confinement Fusion Program, Review of the Department of Energy's Inertial Confinement Fusion Program: The National Ignition Facility, (The National Academies Press, Washington, DC, 1997).

13. D. L. Bleuel, C. B. Yeamans, L. A. Bernstein, R. M. Bionta, J. A. Caggiano, D. T. Casey, G. W. Cooper, O. B. Drury, J. A. Frenje, C. A. Hagmann, R. Hatarik, J. P. Knauer, M. G. Johnson, K. M. Knittel, R. J. Leeper, J. M. McNaney, M. Moran, C. L. Ruiz and D. H. G. Schneider, Rev. Sci. Instrum. **83** (10) (2012).
14. R. M. Bionta, G. P. Grim, K. D. Hahn, E. P. Hartouni, E. A. Henry, H. Y. Khater, A. S. Moore and D. J. Schlossberg, Rev. Sci. Instrum. **92** (4) (2021).
15. S. H. Batha, Rev. Sci. Instrum. **95** (1), 010401 (2024).
16. J. H. Nuckolls, *Contributions to the Genesis and Progress of ICF*. (Inertial confinement nuclear fusion : a historical approach by its pioneers, London, U.K. : Foxwell & Davies (UK), 2007,Ch.1, p1-48, United States, 2006).
17. H. G. Ahlstrom, L. W. Coleman, F. Rienecker Jr. and V. W. Slivinsky, J. Opt. Soc. Am. **68** (12), 1731-1741 (1978).
18. R. L. Kauffman, L. J. Suter, C. B. Darrow, J. D. Kilkenny, H. N. Kornblum, D. S. Montgomery, D. W. Phillion, M. D. Rosen, A. R. Theissen, R. J. Wallace and F. Ze, Phys. Rev. Lett. **73** (17), 2320-2323 (1994).
19. C. Decker, R. E. Turner, O. L. Landen, L. J. Suter, P. Amendt, H. N. Kornblum, B. A. Hammel, T. J. Murphy, J. Wallace, N. D. Delamater, P. Gobby, A. A. Hauer, G. R. Magelssen, J. A. Oertel, J. Knauer, F. J. Marshall, D. Bradley, W. Seka and J. M. Soures, Phys. Rev. Lett. **79** (8), 1491-1494 (1997).
20. S. H. Glenzer, B. J. MacGowan, N. B. Meezan, P. A. Adams, J. B. Alfonso, E. T. Alger, Z. Alherz, L. F. Alvarez, S. S. Alvarez, P. V. Amick, K. S. Andersson, S. D. Andrews, G. J. Antonini, P. A. Arnold, D. P. Atkinson, L. Auyang, S. G. Azevedo, B. N. M. Balaoing, J. A. Baltz, F. Barbosa, G. W. Bardsley, D. A. Barker, A. I. Barnes, A. Baron, R. G. Beeler, B. V. Beeman, L. R. Belk, J. C. Bell, P. M. Bell, R. L. Berger, M. A. Bergonia, L. J. Bernardez, L. V. Berzins, R. C. Bettenhausen, L. Bezerides, S. D. Bhandarkar, C. L. Bishop, E. J. Bond, D. R. Bopp, J. A. Borgman, J. R. Bower, G. A. Bowers, M. W. Bowers, D. T. Boyle, D. K. Bradley, J. L. Bragg, J. Braucht, D. L. Brinkerhoff, D. F. Browning, G. K. Brunton, S. C. Burkhart, S. R. Burns, K. E. Burns, B. Burr, L. M. Burrows, R. K. Butlin, N. J. Cahayag, D. A. Callahan, P. S. Cardinale, R. W. Carey, J. W. Carlson, A. D. Casey, C. Castro, J. R. Celeste, A. Y. Chakicherla, F. W. Chambers, C. Chan, H. Chandrasekaran, C. Chang, R. F. Chapman, K. Charron, Y. Chen, M. J. Christensen, A. J. Churby, T. J. Clancy, B. D. Cline, L. C. Clowdus, D. G. Cocherell, F. E. Coffield, S. J. Cohen, R. L. Costa, J. R. Cox, G. M. Curnow, M. J. Dailey, P. M. Danforth, R. Darbee, P. S. Datte, J. A. Davis, G. A. Deis, R. D. Demaret, E. L. Dewald, P. Di Nicola, J. M. Di Nicola, L. Divol, S. Dixit, D. B. Dobson, T. Doppner, J. D. Driscoll, J. Dugorepec, J. J. Duncan, P. C. Dupuy, E. G. Dzenitis, M. J. Eckart, S. L. Edson, G. J. Edwards, M. J. Edwards, O. D. Edwards, P. W. Edwards, J. C. Ellefson, C. H. Ellerbee, G. V. Erbert, C. M. Estes, W. J. Fabyan, R. N. Fallejo, M. Fedorov, B. Felker, J. T. Fink, M. D. Finney, L. F. Finnie, M. J. Fischer, J. M. Fisher, B. T. Fishler, J. W. Florio, A. Forsman, C. B. Foxworthy, R. M. Franks, T. Frazier, G. Frieder, T. Fung, G. N. Gawinski, C. R. Gibson, E. Giraldez, S. M. Glenn, B. P. Golick, H. Gonzales, S. A. Gonzales, M. J. Gonzalez, K. L. Griffin, J. Grippen, S. M. Gross, P. H. Gschweng, G. Gururangan, K. Gu, S. W. Haan, S. R. Hahn, B. J. Haid, J. E. Hamblen, B. A. Hammel, A. V. Hamza, D. L. Hardy, D. R. Hart, R. G. Hartley, C. A. Haynam, G. M. Heestand, M. R. Hermann, G. L. Hermes, D. S. Hey, R. L. Hibbard, D. G. Hicks, D. E. Hinkel, D. L. Hipple, J. D. Hitchcock, D. L. Hodtwalker, J. P. Holder, J. D. Hollis, G. M. Holtmeier, S. R. Huber, A. W. Huey, D. N. Hulsey, S. L. Hunter, T. R. Huppler, M. S. Hutton, N. Izumi, J. L. Jackson, M. A. Jackson, K. S. Jancaitis, D. R. Jedlovec, B. Johnson, M. C. Johnson, T.

Johnson, M. P. Johnston, O. S. Jones, D. H. Kalantar, J. H. Kamperschroer, R. L. Kauffman, G. A. Keating, L. M. Kegelmeyer, S. L. Kenitzer, J. R. Kimbrough, K. King, R. K. Kirkwood, J. L. Klingmann, K. M. Knittel, T. R. Kohut, K. G. Koka, S. W. Kramer, J. E. Krammen, K. G. Krauter, G. W. Krauter, E. K. Krieger, J. J. Kroll, K. N. La Fortune, L. J. Lagin, V. K. Lakamsani, O. L. Landen, S. W. Lane, A. B. Langdon, S. H. Langer, N. Lao, D. W. Larson, D. Latray, G. T. Lau, S. Le Pape, B. L. Lechleiter, Y. Lee, T. L. Lee, J. Li, J. A. Liebman, J. D. Lindl, S. F. Locke, H. K. Loey, R. A. London, F. J. Lopez, D. M. Lord, R. R. Lowe-Webb, J. G. Lown, A. P. Ludwigsen, N. W. Lum, R. R. Lyons, T. Ma, A. J. MacKinnon, M. D. Magat, D. T. Maloy, T. N. Malsbury, G. Markham, R. M. Marquez, A. A. Marsh, C. D. Marshall, S. R. Marshall, I. L. Maslennikov, D. G. Mathisen, G. J. Mauger, M. Y. Mauvais, J. A. McBride, T. McCarville, J. B. McCloud, A. McGrew, B. McHale, A. G. MacPhee, J. F. Meeker, J. S. Merill, E. P. Mertens, P. A. Michel, M. G. Miller, T. Mills, J. L. Milovich, R. Miramontes, R. C. Montesanti, M. M. Montoya, J. Moody, J. D. Moody, K. A. Moreno, J. Morris, K. M. Morriston, J. R. Nelson, M. Neto, J. D. Neumann, E. Ng, Q. M. Ngo, B. L. Olejniczak, R. E. Olson, N. L. Orsi, M. W. Owens, E. H. Padilla, T. M. Pannell, T. G. Parham, R. W. Patterson, G. Pavel, R. R. Prasad, D. Pendlton, F. A. Penko, B. L. Pepmeier, D. E. Petersen, T. W. Phillips, D. Pigg, K. W. Piston, K. D. Pletcher, C. L. Powell, H. B. Radousky, B. S. Raimondi, J. E. Ralph, R. L. Rampke, R. K. Reed, W. A. Reid, V. V. Rekow, J. L. Reynolds, J. J. Rhodes, M. J. Richardson, R. J. Rinnert, B. P. Riordan, A. S. Rivenes, A. T. Rivera, C. J. Roberts, J. A. Robinson, R. B. Robinson, S. R. Robison, O. R. Rodriguez, S. P. Rogers, M. D. Rosen, G. F. Ross, M. Runkel, A. S. Runtal, R. A. Sacks, S. F. Sailors, J. T. Salmon, J. D. Salmonson, R. L. Saunders, J. R. Schaffer, T. M. Schindler, M. J. Schmitt, M. B. Schneider, K. S. Segraves, M. J. Shaw, M. E. Sheldrick, R. T. Shelton, M. K. Shiflett, S. J. Shiromizu, M. Shor, L. L. Silva, S. A. Silva, K. M. Skulina, D. A. Smauley, B. E. Smith, L. K. Smith, A. L. Solomon, S. Sommer, J. G. Soto, N. I. Spafford, D. E. Speck, P. T. Springer, M. Stadermann, F. Stanley, T. G. Stone, E. A. Stout, P. L. Stratton, R. J. Strausser, L. J. Suter, W. Sweet, M. F. Swisher, J. D. Tappero, J. B. Tassano, J. S. Taylor, E. A. Tekle, C. Thai, C. A. Thomas, A. Thomas, A. L. Throop, G. L. Tietbohl, J. M. Tillman, R. P. J. Town, S. L. Townsend, K. L. Tribbey, D. Trummer, J. Truong, J. Vaher, M. Valadez, P. Van Arsdall, A. J. Van Prooyen, E. O. V. de Dios, M. D. Vergino, S. P. Vernon, J. L. Vickers, G. T. Villanueva, M. A. Vitalich, S. A. Vonhof, F. E. Wade, R. J. Wallace, C. T. Warren, A. L. Warrick, J. Watkins, S. Weaver, P. J. Wegner, M. A. Weingart, J. Wen, K. S. White, P. K. Whitman, K. Widmann, C. C. Widmayer, K. Wilhelmsen, E. A. Williams, W. H. Williams, L. Willis, E. F. Wilson, B. A. Wilson, M. C. Witte, K. Work, P. S. Yang, B. K. Young, K. P. Youngblood, R. A. Zacharias, T. Zaleski, P. G. Zapata, H. Zhang, J. S. Zielinski, J. L. Kline, G. A. Kyrala, C. Niemann, J. D. Kilkenny, A. Nikroo, B. M. Van Wonterghem, L. J. Atherton and E. I. Moses, Phys. Rev. Lett. **106** (8) (2011).

21. J. D. Moody, D. A. Callahan, D. E. Hinkel, P. A. Amendt, K. L. Baker, D. Bradley, P. M. Celliers, E. L. Dewald, L. Divol, T. Döppner, D. C. Eder, M. J. Edwards, O. Jones, S. W. Haan, D. Ho, L. B. Hopkins, N. Izumi, D. Kalantar, R. L. Kauffman, J. D. Kilkenny, O. Landen, B. Lasinski, S. LePape, T. Ma, B. J. MacGowan, S. A. MacLaren, A. J. Mackinnon, D. Meeker, N. Meezan, P. Michel, J. L. Milovich, D. Munro, A. E. Pak, M. Rosen, J. Ralph, H. F. Robey, J. S. Ross, M. B. Schneider, D. Strozzi, E. Storm, C. Thomas, R. P. J. Town, K. L. Widmann, J. Kline, G. Kyrala, A. Nikroo, T. Boehly, A. S. Moore and S. H. Glenzer, Phys. Plasmas **21** (5) (2014).

22. L. J. Suter, A. A. Hauer, L. V. Powers, D. B. Ress, N. Delameter, W. W. Hsing, O. L. Landen, A. R. Thiessen and R. E. Turner, Phys. Rev. Lett. **73** (17), 2328-2331 (1994).

23. P. Michel, L. Divol, E. A. Williams, S. Weber, C. A. Thomas, D. A. Callahan, S. W. Haan, J. D. Salmonson, S. Dixit, D. E. Hinkel, M. J. Edwards, B. J. MacGowan, J. D. Lindl, S. H. Glenzer and L. J. Suter, Phys. Rev. Lett. **102** (2), 025004 (2009).
24. N. D. Delamater, G. R. Magelssen and A. A. Hauer, Phys. Rev. E **53** (5), 5240-5248 (1996).
25. E. L. Dewald, J. L. Milovich, P. Michel, O. L. Landen, J. L. Kline, S. Glenn, O. Jones, D. H. Kalantar, A. Pak, H. F. Robey, G. A. Kyrala, L. Divol, L. R. Benedetti, J. Holder, K. Widmann, A. Moore, M. B. Schneider, T. Döppner, R. Tommasini, D. K. Bradley, P. Bell, B. Ehrlich, C. A. Thomas, M. Shaw, C. Widmayer, D. A. Callahan, N. B. Meezan, R. P. J. Town, A. Hamza, B. Dzenitis, A. Nikroo, K. Moreno, B. Van Wonterghem, A. J. Mackinnon, S. H. Glenzer, B. J. MacGowan, J. D. Kilkenny, M. J. Edwards, L. J. Atherton and E. I. Moses, Phys. Rev. Lett. **111** (23) (2013).
26. T. R. Boehly, D. Munro, P. M. Celliers, R. E. Olson, D. G. Hicks, V. N. Goncharov, G. W. Collins, H. F. Robey, S. X. Hu, J. A. Morozas, T. C. Sangster, O. L. Landen and D. D. Meyerhofer, Phys. Plasmas **16** (5) (2009).
27. H. F. Robey, P. M. Celliers, J. D. Moody, J. Sater, T. Parham, B. Kozioziemski, R. Dylla-Spears, J. S. Ross, S. LePape, J. E. Ralph, M. Hohenberger, E. L. Dewald, L. B. Hopkins, J. J. Kroll, B. E. Yoxall, A. V. Hamza, T. R. Boehly, A. Nikroo, O. L. Landen and M. J. Edwards, Phys. Plasmas **21** (2) (2014).
28. D. H. Munro, P. M. Celliers, G. W. Collins, D. M. Gold, L. B. Da Silva, S. W. Haan, R. C. Cauble, B. A. Hammel and W. W. Hsing, Phys. Plasmas **8** (5 PT2), 2245-2250 (2001).
29. J. D. Moody, H. F. Robey, P. M. Celliers, D. H. Munro, D. A. Barker, K. L. Baker, T. Doppner, N. L. Hash, L. B. Hopkins, K. LaFortune, O. L. Landen, S. LePape, B. J. MacGowan, J. E. Ralph, J. S. Ross, C. Widmayer, A. Nikroo, E. Giraldez and T. Boehly, Phys. Plasmas **21** (9) (2014).
30. H. F. Robey, T. R. Boehly, P. M. Celliers, J. H. Eggert, D. Hicks, R. F. Smith, R. Collins, M. W. Bowers, K. G. Krauter, P. S. Datte, D. H. Munro, J. L. Milovich, O. S. Jones, P. A. Michel, C. A. Thomas, R. E. Olson, S. Pollaine, R. P. J. Town, S. Haan, D. Callahan, D. Clark, J. Edwards, J. L. Kline, S. Dixit, M. B. Schneider, E. L. Dewald, K. Widmann, J. D. Moody, T. Döppner, H. B. Radousky, A. Throop, D. Kalantar, P. DiNicola, A. Nikroo, J. J. Kroll, A. V. Hamza, J. B. Horner, S. D. Bhandarkar, E. Dzenitis, E. Alger, E. Giraldez, C. Castro, K. Moreno, C. Haynam, K. N. LaFortune, C. Widmayer, M. Shaw, K. Jancaitis, T. Parham, D. M. Holunga, C. F. Walters, B. Haid, E. R. Mapoles, J. Sater, C. R. Gibson, T. Malsbury, J. Fair, D. Trummer, K. R. Coffee, B. Burr, L. V. Berzins, C. Choate, S. J. Brereton, S. Azevedo, H. Chandrasekaran, D. C. Eder, N. D. Masters, A. C. Fisher, P. A. Sterne, B. K. Young, O. L. Landen, B. M. Van Wonterghem, B. J. MacGowan, J. Atherton, J. D. Lindl, D. D. Meyerhofer and E. Moses, Phys. Plasmas **19** (4), 042706 (2012).
31. S. Bhandarkar, J. Fair, B. Haid, E. Mapoles, J. Atherton, C. Thomas, J. Moody, J. Kroll and A. Nikroo, Fusion Sci. Technol. **73** (3), 380-391 (2018).
32. D. G. Hicks, B. K. Spears, D. G. Braun, R. E. Olson, C. M. Sorce, P. M. Celliers, G. W. Collins and O. L. Landen, Rev. Sci. Instrum. **81** (10) (2010).
33. M. A. Barrios, S. P. Regan, L. J. Suter, S. Glenn, L. R. Benedetti, D. K. Bradley, G. W. Collins, R. Epstein, B. A. Hammel, G. A. Kyrala, N. Izumi, T. Ma, H. Scott and V. A. Smalyuk, Phys. Plasmas **20** (7), 072706 (2013).
34. S. P. Regan, R. Epstein, B. A. Hammel, L. J. Suter, H. A. Scott, M. A. Barrios, D. K. Bradley, D. A. Callahan, C. Cerjan, G. W. Collins, S. N. Dixit, T. Doppner, M. J. Edwards, D. R. Farley, K. B. Fournier, S. Glenn, S. H. Glenzer, I. E. Golovkin, S. W. Haan, A. Hamza, D. G. Hicks, N. Izumi, O. S. Jones, J. D. Kilkenny, J. L. Kline, G. A. Kyrala, O. L. Landen, T. Ma, J. J. MacFarlane, A. J.

MacKinnon, R. C. Mancini, R. L. McCrory, N. B. Meezan, D. D. Meyerhofer, A. Nikroo, H. S. Park, J. Ralph, B. A. Remington, T. C. Sangster, V. A. Smalyuk, P. T. Springer and R. P. J. Town, Phys. Rev. Lett. **111** (4) (2013).
35. T. Ma, P. K. Patel, N. Izumi, P. T. Springer, M. H. Key, L. J. Atherton, L. R. Benedetti, D. K. Bradley, D. A. Callahan, P. M. Celliers, C. J. Cerjan, D. S. Clark, E. L. Dewald, S. N. Dixit, T. Döppner, D. H. Edgell, R. Epstein, S. Glenn, G. Grim, S. W. Haan, B. A. Hammel, D. Hicks, W. W. Hsing, O. S. Jones, S. F. Khan, J. D. Kilkenny, J. L. Kline, G. A. Kyrala, O. L. Landen, S. Le Pape, B. J. MacGowan, A. J. Mackinnon, A. G. MacPhee, N. B. Meezan, J. D. Moody, A. Pak, T. Parham, H. S. Park, J. E. Ralph, S. P. Regan, B. A. Remington, H. F. Robey, J. S. Ross, B. K. Spears, V. Smalyuk, L. J. Suter, R. Tommasini, R. P. Town, S. V. Weber, J. D. Lindl, M. J. Edwards, S. H. Glenzer and E. I. Moses, Phys. Rev. Lett. **111** (8), 085004 (2013).
36. O. L. Landen, D. T. Casey, J. M. DiNicola, T. Doeppner, E. P. Hartouni, D. E. Hinkel, L. F. Berzak Hopkins, M. Hohenberger, A. L. Kritcher, S. LePape, B. J. MacGowan, S. Maclaren, K. D. Meaney, M. Millot, P. K. Patel, J. Park, L. A. Pickworth, H. F. Robey, J. S. Ross, S. T. Yang, A. B. Zylstra, K. L. Baker, D. A. Callahan, P. M. Celliers, M. J. Edwards, O. A. Hurricane, J. D. Lindl, J. D. Moody, J. Ralph, V. A. Smalyuk, C. A. Thomas, B. M. Van Wonterghem and C. R. Weber, High Energy Dens. Phys. **36**, 100755 (2020).
37. A. G. MacPhee, J. L. Peterson, D. T. Casey, D. S. Clark, S. W. Haan, O. S. Jones, O. L. Landen, J. L. Milovich, H. F. Robey and V. A. Smalyuk, Phys. Plasmas **22** (8) (2015).
38. K. S. Raman, V. A. Smalyuk, D. T. Casey, S. W. Haan, D. E. Hoover, O. A. Hurricane, J. J. Kroll, A. Nikroo, J. L. Peterson, B. A. Remington, H. F. Robey, D. S. Clark, B. A. Hammel, O. L. Landen, M. M. Marinak, D. H. Munro, K. J. Peterson and J. Salmonson, Phys. Plasmas **21** (7), 072710 (2014).
39. A. J. MacKinnon, N. B. Meezan, J. S. Ross, S. Le Pape, L. Berzak Hopkins, L. Divol, D. Ho, J. Milovich, A. Pak, J. Ralph, T. Döppner, P. K. Patel, C. Thomas, R. Tommasini, S. Haan, A. G. MacPhee, J. McNaney, J. Caggiano, R. Hatarik, R. Bionta, T. Ma, B. Spears, J. R. Rygg, L. R. Benedetti, R. P. J. Town, D. K. Bradley, E. L. Dewald, D. Fittinghoff, O. S. Jones, H. R. Robey, J. D. Moody, S. Khan, D. A. Callahan, A. Hamza, J. Biener, P. M. Celliers, D. G. Braun, D. J. Erskine, S. T. Prisbrey, R. J. Wallace, B. Kozioziemski, R. Dylla-Spears, J. Sater, G. Collins, E. Storm, W. Hsing, O. Landen, J. L. Atherton, J. D. Lindl, M. J. Edwards, J. A. Frenje, M. Gatu-Johnson, C. K. Li, R. Petrasso, H. Rinderknecht, M. Rosenberg, F. H. Séguin, A. Zylstra, J. P. Knauer, G. Grim, N. Guler, F. Merrill, R. Olson, G. A. Kyrala, J. D. Kilkenny, A. Nikroo, K. Moreno, D. E. Hoover, C. Wild and E. Werner, Phys. Plasmas **21** (5), 056318 (2014).
40. S. Le Pape, L. F. Hopkins, L. Divol, A. Pak, E. Dewald, S. Bhandarkar, L. R. Bennedetti, T. Bunn, J. Biener, J. Crippen, D. Casey, D. Edgell, D. Fittinghoff, M. Gatu-Johnson, C. Goyon, S. Haan, R. Hatarik, M. Havre, D. Ho and O. Hurricane, Phys. Rev. Lett. **120** (2018).
41. L. Divol, A. Pak, L. F. B. Hopkins, S. Le Pape, N. B. Meezan, E. L. Dewald, D. D. M. Ho, S. F. Khan, A. J. Mackinnon, J. S. Ross, D. P. Turnbull, C. Weber, P. M. Celliers, M. Millot, L. R. Benedetti, J. E. Field, N. Izumi, G. A. Kyrala, T. Ma, S. R. Nagel, J. R. Rygg, D. Edgell, A. G. Macphee, C. Goyon, M. Hohenberger, B. J. MacGowan, P. Michel, D. Strozzi, W. S. Cassata, D. Casey, D. N. Fittinghoff, N. Gharibyan, R. Hatarik, D. Sayre, P. Volegov, C. Yeamans, B. Bachmann, T. Döppner, J. Biener, J. Crippen, C. Choate, H. Huang, C. Kong, A. Nikroo, N. G. Rice, M. Stadermann, S. D. Bhandarkar, S. Haan, B. Kozioziemski, W. W. Hsing, O. L. Landen, J. D. Moody, R. P. J. Town, D. A. Callahan, O. A. Hurricane and M. J. Edwards, Phys. Plasmas **24** (5) (2017).

42. K. L. Baker, C. A. Thomas, D. T. Casey, S. Khan, B. K. Spears, R. Nora, T. Woods, J. L. Milovich, R. L. Berger, D. Strozzi, D. Clark, M. Hohenberger, O. A. Hurricane, D. A. Callahan, O. L. Landen, B. Bachmann, R. Benedetti, R. Bionta, P. M. Celliers, D. Fittinghoff, C. Goyon, G. Grim, R. Hatarik, N. Izumi, M. Gatu Johnson, G. Kyrala, T. Ma, M. Millot, S. R. Nagel, A. Pak, P. K. Patel, D. Turnbull, P. L. Volegov and C. Yeamans, Phys. Rev. Lett. **121** (13), 135001 (2018).
43. D. T. Casey, C. A. Thomas, K. L. Baker, B. K. Spears, M. Hohenberger, S. F. Khan, R. C. Nora, C. R. Weber, D. T. Woods, O. A. Hurricane, D. A. Callahan, R. L. Berger, J. L. Milovich, P. K. Patel, T. Ma, A. Pak, L. R. Benedetti, M. Millot, C. Jarrott, O. L. Landen, R. M. Bionta, B. J. MacGowan, D. J. Strozzi, M. Stadermann, J. Biener, A. Nikroo, C. S. Goyon, N. Izumi, S. R. Nagel, B. Bachmann, P. L. Volegov, D. N. Fittinghoff, G. P. Grim, C. B. Yeamans, M. Gatu Johnson, J. A. Frenje, N. Rice, C. Kong, J. Crippen, J. Jaquez, K. Kangas and C. Wild, Phys. Plasmas **25** (5), 056308 (2018).
44. J. R. Rygg, O. S. Jones, J. E. Field, M. A. Barrios, L. R. Benedetti, G. W. Collins, D. C. Eder, M. J. Edwards, J. L. Kline, J. J. Kroll, O. L. Landen, T. Ma, A. Pak, J. L. Peterson, K. Raman, R. P. J. Town and D. K. Bradley, Phys. Rev. Lett. **112** (19) (2014).
45. S. R. Nagel, S. W. Haan, J. R. Rygg, M. Barrios, L. R. Benedetti, D. K. Bradley, J. E. Field, B. A. Hammel, N. Izumi, O. S. Jones, S. F. Khan, T. Ma, A. E. Pak, R. Tommasini and R. P. J. Town, Phys. Plasmas **22** (2) (2015).
46. R. Tommasini, J. E. Field, B. A. Hammel, O. L. Landen, S. W. Haan, C. Aracne-Ruddle, L. R. Benedetti, D. K. Bradley, D. A. Callahan, E. L. Dewald, T. Doeppner, M. J. Edwards, O. A. Hurricane, N. Izumi, O. A. Jones, T. Ma, N. B. Meezan, S. R. Nagel, J. R. Rygg, K. S. Segraves, M. Stadermann, R. J. Strauser and R. P. J. Town, Phys. Plasmas **22** (5) (2015).
47. B. Bachmann, J. E. Ralph, A. B. Zylstra, S. A. MacLaren, T. Döppner, D. O. Gericke, G. W. Collins, O. A. Hurricane, T. Ma, J. R. Rygg, H. A. Scott, S. A. Yi and P. K. Patel, Phys. Rev. E **101** (3), 033205 (2020).
48. A. Pak, L. Divol, C. R. Weber, L. F. B. Hopkins, D. S. Clark, E. L. Dewald, D. N. Fittinghoff, V. Geppert-Kleinrath, M. Hohenberger, S. Le Pape, T. Ma, A. G. MacPhee, D. A. Mariscal, E. Marley, A. S. Moore, L. A. Pickworth, P. L. Volegov, C. Wilde, O. A. Hurricane and P. K. Patel, Phys. Rev. Lett. **124** (14) (2020).
49. A. B. Zylstra, C. Yeamans, S. Le Pape, A. MacKinnon, M. Hohenberger, D. N. Fittinghoff, H. Herrmann, Y. Kim, P. B. Radha, P. W. McKenty, R. S. Craxton and M. Hoppe, Phys. Plasmas **27** (12) (2020).
50. P. L. Volegov, (2019).
51. L. A. Pickworth, A. Smalyuk, B. A. Hammel, C. Weber, D. S. Clark, H. F. Robey, A. G. MacPhee, S. Le Pape, D. T. Casey, L. Berzak-Hopkins, A. Zylstra, A. Kritcher, C. F. Walters, S. D. Bhandarkar, M. Stadermann, S. Johnson, S. Diaz, M. Ratledge, N. Alfonso, O. N. Landen, A. E. Pak, N. Izumi, S. F. Khan, L. R. Benedetti, B. Lahmann and E. Hartouni, High Energy Dens. Phys. **37** (2020).
52. A. S. Moore, D. J. Schlossberg, B. D. Appelbe, G. A. Chandler, A. J. Crilly, M. J. Eckart, C. J. Forrest, V. Y. Glebov, G. P. Grim, E. P. Hartouni, R. Hatarik, S. M. Kerr, J. Kilkenny and J. P. Knauer, Rev. Sci. Instrum. **94** (6) (2023).
53. D. J. Schlossberg, G. P. Grim, D. T. Casey, A. S. Moore, R. Nora, B. Bachmann, L. R. Benedetti, R. M. Bionta, M. J. Eckart, J. E. Field, D. N. Fittinghoff, M. G. Johnson, V. Geppert-Kleinrath, E. P. Hartouni, R. Hatarik, W. W. Hsing, L. C. Jarrott, S. F. Khan, J. D. Kilkenny, O. L.

Landen, B. J. MacGowan, A. J. Mackinnon, K. D. Meaney, D. H. Munro, S. R. Nagel, A. Pak, P. K. Patel, B. K. Spears, P. L. Volegov and C. V. Young, Phys. Rev. Lett. **127** (12) (2021).
54. B. J. MacGowan, O. L. Landen, D. T. Casey, C. V. Young, D. A. Callahan, E. P. Hartouni, R. Hatarik, M. Hohenberger, T. Ma, D. Mariscal, A. Moore, R. Nora, H. G. Rinderknecht, D. Schlossberg and B. M. Van Wonterghem, High Energy Dens. Phys. **40**, 100944 (2021).
55. H. G. Rinderknecht, D. T. Casey, R. Hatarik, R. M. Bionta, B. J. MacGowan, P. Patel, O. L. Landen, E. P. Hartouni and O. A. Hurricane, Phys. Rev. Lett. **124** (14), 145002 (2020).
56. O. A. Hurricane, D. T. Casey, O. Landen, A. L. Kritcher, R. Nora, P. K. Patel, J. A. Gaffney, K. D. Humbird, J. E. Field, M. K. G. Kruse, J. L. Peterson and B. K. Spears, Phys. Plasmas **27** (6) (2020).
57. D. T. Casey, B. J. MacGowan, J. D. Sater, A. B. Zylstra, O. L. Landen, J. Milovich, O. A. Hurricane, A. L. Kritcher, M. Hohenberger, K. Baker, S. Le Pape, T. Döppner, C. Weber, H. Huang, C. Kong, J. Biener, C. V. Young, S. Haan, R. C. Nora, S. Ross, H. Robey, M. Stadermann, A. Nikroo, D. A. Callahan, R. M. Bionta, K. D. Hahn, A. S. Moore, D. Schlossberg, M. Bruhn, K. Sequoia, N. Rice, M. Farrell and C. Wild, Phys. Rev. Lett. **126** (2), 025002 (2021).
58. A. Pak, L. Divol, D. T. Casey, S. F. Khan, A. L. Kritcher, J. E. Ralph, R. Tommasini, C. Trosseille, A. B. Zylstra, K. L. Baker, N. W. Birge, R. Bionta, B. Bachmann, E. L. Dewald, T. Doeppner, M. S. Freeman, D. N. Fittinghoff, V. Geppert-Kleinrath, H. Geppert-Kleinrath, K. D. Hahn, M. Hohenberger, J. Holder, S. Kerr, Y. Kim, B. Kozioziemski, K. Lamb, B. J. MacGowan, A. G. MacPhee, K. D. Meaney, A. S. Moore, D. J. Schlossberg, S. Stoupin, P. Volegov, C. Wilde, C. V. Young, O. L. Landen and R. P. J. Town, Phys. Rev. Lett. **131** (6), 065101 (2023).
59. M. S. Rubery, M. D. Rosen, N. Aybar, O. L. Landen, L. Divol, C. V. Young, C. Weber, J. Hammer, J. D. Moody, A. S. Moore, A. L. Kritcher, A. B. Zylstra, O. Hurricane, A. E. Pak, S. MacLaren, G. Zimmerman, J. Harte and T. Woods, Phys. Rev. Lett. **132** (6), 065104 (2024).